

# Prediction of Induced Voltages on Ports in Complex, Three-Dimensional Enclosures With Apertures, Using the Random Coupling Model

Jesus Gil Gil, Zachary B. Drikas, *Member, IEEE*, Tim D. Andreadis, and Steven M. Anlage, *Member, IEEE*

**Abstract**—A statistical modeling technique known as the random coupling model (RCM) is an effective method for estimating the probabilistic magnitudes of induced voltages on objects within a closed, complex, three-dimensional (3-D) enclosure. The limitations of the RCM to predict electromagnetic wave coupling into an enclosure with apertures are examined. We experimentally demonstrate the applicability of the RCM to estimate the probabilistic magnitudes of voltages induced on ports in a complex 3-D enclosure with an electrically large aperture. This study is a first step toward being able to predict effects on sensitive electronic targets in large, real-world, lossy enclosures such as office buildings, ship compartments, and aircraft compartments.

**Index Terms**—Aperture antennas, electromagnetic compatibility, overmoded enclosures, probability density function (PDF), random coupling model (RCM), statistical electromagnetism, wave scattering.

## I. INTRODUCTION

THE random coupling model (RCM) makes predictions of induced voltages on ports of interest (e.g., sensitive electronics) in wave-chaotic enclosures. There are many approaches to the statistical study of electromagnetics in enclosures [1]–[7], which include both field-based methods and microwave network methods. The RCM uses impedance parameters of an enclosure and its ports as well as an additional parameter called the loss parameter to calculate induced voltage statistics on ports in the enclosure (this process is described in Section II). These ports can be monopole antennas, pins on an integrated circuit, apertures, or wires or bundles of wires running inside a below-deck ship compartment [8], [9]. The RCM allows the determination of the probability density function (PDF) of induced voltages on a port of interest in an enclosure. The RCM results are independent of specific cavity configurations relying only on the port characteristics and the loss parameter.

Both the theory and original experimental work on the RCM were carried out by researchers at the University of Maryland (UMD), where their experimental work focused primarily on quasi-two-dimensional (2-D) cavities, and a small 3-D enclosure with apertures (computer box) [10]–[12]. Through this paper, it has been conclusively shown that the RCM accurately predicts

induced voltages in the closed, complex enclosures they studied. Additional experimental work performed by researchers at the Naval Research Laboratory in collaboration with the UMD has verified the RCM for larger closed cavities [8]. This paper will show that the RCM can also be applied to determine the PDFs of induced voltages on ports of interest in enclosures with electrically large apertures when radiation occurs internally to the enclosure.

The RCM requires the enclosure to be ray-chaotic, reverberant, and have a characteristic length (cube root of the volume)  $L$  that is  $\gtrsim 3\lambda$  [13]. A ray-chaotic enclosure (schematically shown in Fig. 1) has complex-shaped boundaries or objects which create chaotic ray trajectories. This means that a pair of rays with similar initial conditions will separate rapidly as they bounce around the enclosure, as illustrated in Fig. 1 [13].

The RCM makes use of random matrix theory (RMT) to make statistical predictions. RMT was developed in the 1950's and was applied to the study of the energy levels of large-complicated nuclei. It was discovered that the PDF of the normalized nearest neighbor eigen-energy spacing for different atomic nuclei followed certain universal curves depending only upon whether the classical ray dynamics within the system was integrable or chaotic [12]. It has since been conjectured that RMT is applicable to any wave chaotic system (electromagnetic, acoustic, etc.) [14]. RMT, however, only characterizes ideal systems, namely, one in which the waves entering and leaving the ports are perfectly coupled to the system, i.e., there is no “prompt” reflection at the transmitting port, although there can be “equilibrated” waves leaving there that have entered the system and later returned to the port [13]. In addition, it is assumed that all incident rays entering from a port are subsumed into ray-chaotic trajectories and do not bounce back after executing a “short orbit” [15], [16]. The RCM extends RMT by accounting for the above-mentioned nonuniversal port characteristics of wave-chaotic systems (see Fig. 2), and allows the calculation of PDFs of induced voltages on a receiving port (see port 2 in Fig. 1), due to an incident signal at port 1, under realistic conditions.

## II. THEORY

The RCM can be applied to 2-D and 3-D enclosures with multiple ports [17]. According to this model, the statistics of the induced voltages on a port located inside the enclosure are governed in part by a single quantity, the loss parameter  $\alpha$ , of the enclosure, which is defined as the ratio of the 3 dB bandwidth of a typical cavity mode resonance to the mean spacing between the modes  $\alpha = k^2 / (\Delta k^2 Q)$ . Here,  $k$  is the wavenumber,  $\Delta k^2$  is the mean spacing between  $k^2$  eigenvalues, and  $Q$  is the quality factor of the closed system. The loss parameter determines the

Manuscript received September 18, 2015; revised February 29, 2016; accepted April 14, 2016. Date of publication July 14, 2016; date of current version August 16, 2016.

J. Gil Gil, Z. B. Drikas, and T. D. Andreadis are with the Naval Research Laboratory, Washington, DC 20375-5320 USA (e-mail: jesus.gilgil@nrl.navy.mil; zachary.drikas@nrl.navy.mil; tim.andreadis@nrl.navy.mil).

S. Anlage is with the Department of Physics, University of Maryland, College Park, MD 20742-4111 USA (e-mail: anlage@umd.edu).

Color versions of one or more of the figures in this paper are available online at <http://ieeexplore.ieee.org>.

Digital Object Identifier 10.1109/TEMC.2016.2580301

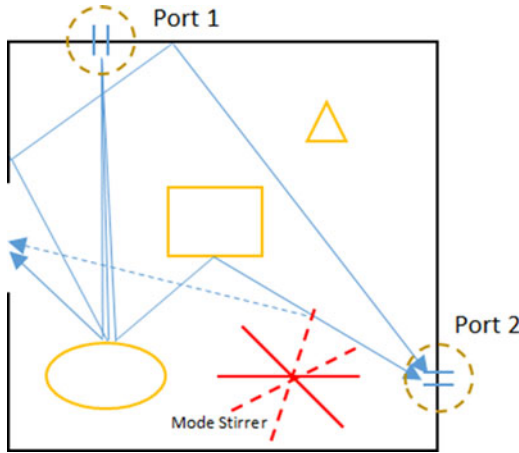


Fig. 1. Ray-chaotic cavities are characterized by rapidly diverging ray trajectories. Three similar initial ray trajectories are shown emerging from port 1, yet they quickly undergo three very different evolutions in the ray-chaotic enclosure. The figure shows a mode stirrer which is used to realized multiple cavity configurations which have the same volume but different detailed ray dynamics

statistics of the universal properties of wave-chaotic systems, and further determining the induced voltage statistics for an enclosure with system-specific real-world port characteristics requires the radiation impedance  $Z_{\text{rad}}$  and the radiated power at the source port. The general expression of the loss parameter for a 3-D enclosure is

$$\alpha = \frac{k^3 V}{2\pi^2 Q} \quad (1)$$

where  $V$  is the volume of the enclosure. This expression has been shown to be valid for enclosures without apertures (low loss) [8], [13], and a number of methods have been used to determine the loss parameter [12]. However, with the introduction of apertures (high loss), the enclosure volume becomes less well defined (imagine a rectangular enclosure with one or more walls removed). In the case of high loss, the determination of the loss parameter must be reexamined, and we do that here. We will show in Section II that the statistics of measured voltages induced on port 2 compare well with the RCM-predicted statistics of induced voltage values for the same port, thus, validating the use of the RCM for high-loss enclosures. The measured induced voltage values are calculated using

$$\bar{V}_2^{\text{exp}} = \left[ \frac{P_{\text{in}} |\bar{Z}_{21}^{\text{cav}}|^2}{\text{Re} \{ \bar{Z}_{11}^{\text{cav}} \}} \right]^{1/2} \quad (2)$$

where  $P_{\text{in}}$  is the input power to port 1, and  $\bar{Z}_{ij}^{\text{cav}}$  are the measured (and fluctuating) impedance parameters of the cavity. The statistical treatment of data begins with measurement of the enclosure (cavity) scattering parameters for a two-port system like that shown in Fig. 1:

$$\bar{\bar{S}}^{\text{cav}} = \begin{bmatrix} \bar{S}_{11}^{\text{cav}} & \bar{S}_{12}^{\text{cav}} \\ \bar{S}_{21}^{\text{cav}} & \bar{S}_{22}^{\text{cav}} \end{bmatrix} \quad (3)$$

which is a matrix quantity (denoted by the double bar) where  $\bar{S}_{ij}^{\text{cav}}$  are complex vectors in frequency ( $i, j \in \{1, 2\}$ ).  $\bar{Z}^{\text{cav}}$  is

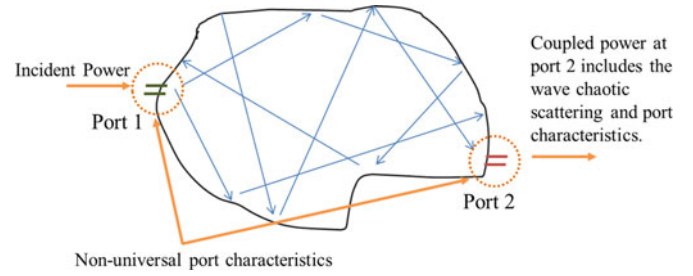


Fig. 2. Idealized wave scattering theories predict the universal statistical properties of wave-chaotic enclosures, but do not account for system-specific port coupling and short orbits. The RCM accounts for the port coupling characteristics and short orbits of specific, real-world enclosures.

then obtained from (3) using the bilinear transformation

$$\bar{\bar{Z}}^{\text{cav}} = \bar{\bar{Z}}_0^{1/2} \left( \bar{\bar{1}} + \bar{\bar{S}}^{\text{cav}} \right) \left( \bar{\bar{1}} - \bar{\bar{S}}^{\text{cav}} \right)^{-1} \bar{\bar{Z}}_0^{1/2} \quad (4)$$

where the real diagonal matrix  $\bar{\bar{Z}}_0$  has elements which are the characteristic impedances of the channels or transmission lines that guide waves to/from the ports, and  $\bar{\bar{1}}$  is the  $2 \times 2$  identity matrix [13]. The measured induced voltage statistics are then calculated using (2).

The RCM-predicted induced voltages are calculated using

$$\bar{V}_2^{\text{RCM}} = \left[ \frac{P_{\text{in}} |\bar{Z}_{21}^{\text{RCM}}|^2}{\text{Re} \{ \bar{Z}_{11}^{\text{RCM}} \}} \right]^{1/2} \quad (5)$$

where  $\bar{Z}_{ij}^{\text{RCM}}$  are the RCM-predicted impedance parameters calculated using the measured radiation impedance of the enclosure ports and the loss parameter of the enclosure. As mentioned, there are several methods for calculating  $\alpha$  (discussed in Section III). We calculate  $\alpha$  using the statistics of the measured ensemble impedance by computing the quantity

$$\alpha_{ij} = \frac{1}{\pi \sigma_{\bar{z}_{\text{norm } ij}^{\text{exp}}}^2} \quad (6)$$

Here,  $i, j \in \{1, 2\}$  and  $\sigma_{\bar{z}_{\text{norm } ij}^{\text{exp}}}$  is the variance of either of the diagonal elements ( $i = j$ ), or the off-diagonal elements ( $i \neq j$ ), of the normalized enclosure impedance. The normalized impedance  $\bar{z}_{\text{norm}}^{\text{exp}}$  is calculated as

$$\bar{z}_{\text{norm}}^{\text{exp}} = \left( \text{Re} \{ \bar{\bar{Z}}^{\text{rad}} \} \right)^{-1/2} \left( \bar{\bar{Z}}^{\text{cav}} - j \text{Im} \{ \bar{\bar{Z}}^{\text{rad}} \} \right) \times \left( \text{Re} \{ \bar{\bar{Z}}^{\text{rad}} \} \right)^{-1/2} \quad (7)$$

Here,  $\bar{\bar{Z}}^{\text{rad}}$  is the radiation impedance matrix of the ports, which characterizes the nonuniversal aspects of the enclosure, and is calculated similarly to (4) as

$$\bar{\bar{Z}}^{\text{rad}} = \bar{\bar{Z}}_0^{1/2} \left( \bar{\bar{1}} + \bar{\bar{S}}^{\text{rad}} \right) \left( \bar{\bar{1}} - \bar{\bar{S}}^{\text{rad}} \right)^{-1} \bar{\bar{Z}}_0^{1/2} \quad (8)$$

where the radiation scattering matrix  $\bar{\bar{S}}^{\text{rad}}$  is well approximated as the ensemble average of 200 different scattering matrices which correspond to different enclosure configurations (each position of the stirrer creates a new enclosure configuration with the same volume, but different boundary conditions) [8]. We call the ensemble average  $\bar{\bar{S}}^{\text{avg}}$  since it contains short orbits

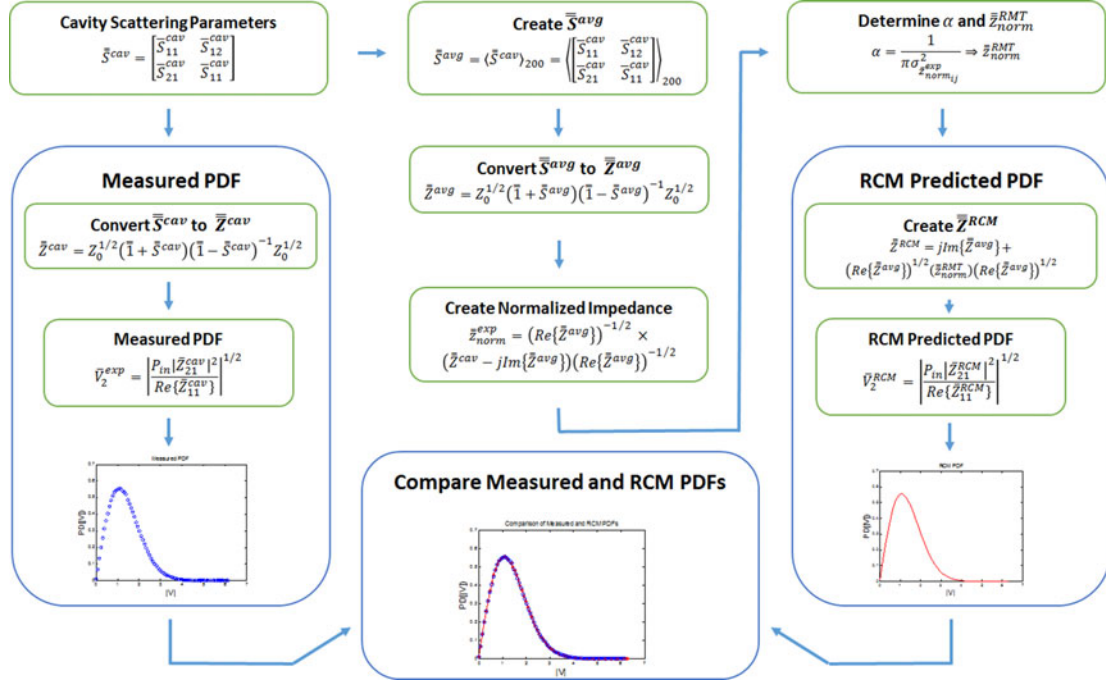


Fig. 3. Data flow diagram of process used to compare measured and RCM-predicted induced voltage statistics.

which  $\bar{S}^{rad}$  does not.  $\bar{S}^{avg}$  can be expressed as

$$\bar{S}^{avg} = \langle \bar{S}^{cav} \rangle_{200} = \left\langle \begin{bmatrix} \bar{S}_{11}^{cav} & \bar{S}_{12}^{cav} \\ \bar{S}_{21}^{cav} & \bar{S}_{22}^{cav} \end{bmatrix} \right\rangle_{200} \quad (9)$$

Now that we have obtained the loss parameter  $\alpha$ , we may calculate the RMT-predicted normalized impedance  $\bar{z}_{norm}^{RMT}$  which will be used to finally calculate  $\bar{Z}^{RCM}$ .  $\bar{z}_{norm}^{RMT}$  is a  $2 \times 2$  complex random matrix, derived from RMT and the loss parameter, and has the form,

$$\bar{z}_{norm}^{RMT} = \begin{bmatrix} Re\{\bar{z}_{norm_{11}}^{RMT}\} + jIm\{\bar{z}_{norm_{11}}^{RMT}\} & Re\{\bar{z}_{norm_{12}}^{RMT}\} + jIm\{\bar{z}_{norm_{12}}^{RMT}\} \\ Re\{\bar{z}_{norm_{21}}^{RMT}\} + jIm\{\bar{z}_{norm_{21}}^{RMT}\} & Re\{\bar{z}_{norm_{22}}^{RMT}\} + jIm\{\bar{z}_{norm_{22}}^{RMT}\} \end{bmatrix} \quad (10)$$

where

$$Re\{\bar{z}_{norm_{11}}^{RMT}\}, Re\{\bar{z}_{norm_{22}}^{RMT}\} \rightarrow N\left(1, \frac{1}{\pi\alpha_{ii}}\right) \quad (11)$$

$$Im\{\bar{z}_{norm_{11}}^{RMT}\}, Im\{\bar{z}_{norm_{22}}^{RMT}\} \rightarrow N\left(0, \frac{1}{\pi\alpha_{ii}}\right) \quad (12)$$

$$Re\{\bar{z}_{norm_{12}}^{RMT}\}, Im\{\bar{z}_{norm_{12}}^{RMT}\} \rightarrow N\left(0, \frac{1}{2\pi\alpha_{ij}}\right) \quad (13)$$

$$Re\{\bar{z}_{norm_{21}}^{RMT}\}, Im\{\bar{z}_{norm_{21}}^{RMT}\} \rightarrow N\left(0, \frac{1}{2\pi\alpha_{ij}}\right). \quad (14)$$

In (11)–(14),  $N(x, y)$  is a Gaussian distribution with mean of  $x$  and variance of  $y$ , and it is assumed that the loss parameter is very large  $\alpha \gg 1$ . Now,  $\bar{Z}^{RCM}$  is calculated using

$$\bar{Z}^{RCM} = jIm\{\bar{Z}^{avg}\} + (Re\{\bar{Z}^{avg}\})^{1/2} \bar{z}_{norm}^{RMT} (Re\{\bar{Z}^{avg}\})^{1/2} \quad (15)$$

and the RCM-predicted induced voltages at port 2 may be calculated using (5). Fig. 3 outlines the above process.

The use of the variance of the normalized impedance of port 1  $\bar{z}_{norm_{11}}^{exp}$  has been thoroughly verified as a valid method for obtaining the loss parameter  $\alpha$  for an enclosure with no apertures [8]. In fact, for such an enclosure, the loss parameters determined from any index combination of  $\bar{z}_{norm_{ij}}^{exp}$  are similar ( $\alpha_{11} \approx \alpha_{22} \approx \alpha_{21}$ ). However, experiments with complex, 3-D enclosures with apertures have shown that the RCM-predicted induced voltage statistics, calculated using  $\alpha$  values obtained using  $\bar{z}_{norm_{11}}^{exp}$  start to deviate from those calculated directly from experimental data. This prompted an evaluation of methods for calculating the loss parameter of a cavity with electrically large apertures.

### III. EXPERIMENTAL SETUP AND DATA ANALYSIS

#### A. Objective and Approach

The objective of the variable aperture experiment is to show that the RCM capability to accurately predict voltages induced on a receiving port is not limited by the aperture size of the enclosure.

A first step toward the stated objective is to verify the accuracy of the RCM in predicting induced voltages in large, complex enclosures with apertures using different methods for obtaining the loss parameter. This is accomplished by constructing the complex aluminum enclosure with dimensions  $1.27 \text{ m} \times 1.22 \text{ m} \times 0.65 \text{ m}$  shown in Fig. 4.

The cavity aperture size is varied while cavity scattering parameters are collected between two interior ports with a vector network analyzer (VNA). The RCM is then applied to the cavity scattering parameters as outlined in the previous section.

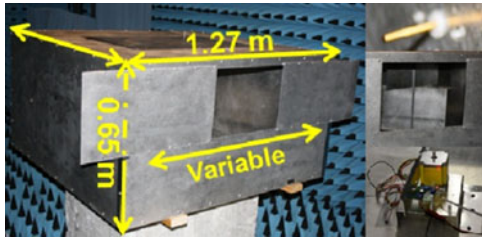


Fig. 4. Test cavity with variable aperture, monopole, stirrer, and stepper motor.

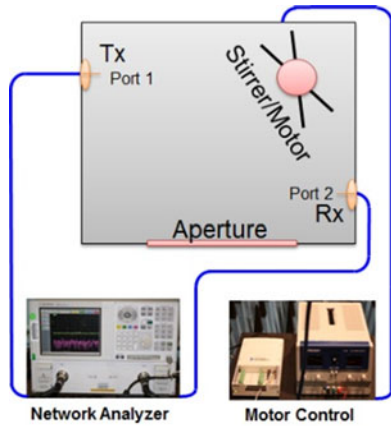


Fig. 5. Variable aperture experimental setup showing a schematic top view of the enclosure, port, mode-stirrer, and aperture locations, and the VNA used to measure the scattering parameters between the two ports.

**B. Experimental Setup**

The enclosure contains two internal ports and has an aperture that can be varied from completely closed to its full aperture opening of 0.31 m × 1.22 m.

The enclosure interior is a mode-stirred chamber with two 1.27 cm long monopole antennas, each acting as a port. The mode-stirrer consists of two 44.5 cm x 30.5 cm plates (one above the other) at 45° to each other, and is rotated by a stepper motor with a minimum stepping increment of 1.8° for a maximum of 200 steps per 360°. An Agilent PNA series VNA is used to collect cavity data in the form of scattering parameters (S-parameters) from each port of the VNA. Transmit power is 0 dBm, and the loss from cables leading to the ports are calibrated out prior to measurement. Fig. 5 details the measurement setup.

A statistical ensemble of data is collected by rotating the stirrer 200 times in 1.8° increments and performing a measurement on each step. Previous experimentation and autocorrelation analysis has shown that 1.8° increments and 200 different stirrer positions is more than sufficient to provide a robust statistical ensemble [8]. The frequency range of interest is 13–14 GHz where the enclosure is highly overmoded and the aperture is within the electrically large limit. Measurements are made in 100 MHz bands, e.g., 13.0–13.1 GHz, 13.1–13.2 GHz, etc.

Experiments were performed with apertures ranging from zero width to the full aperture size of 122 cm x 30.5 cm in 10.16 cm increments.

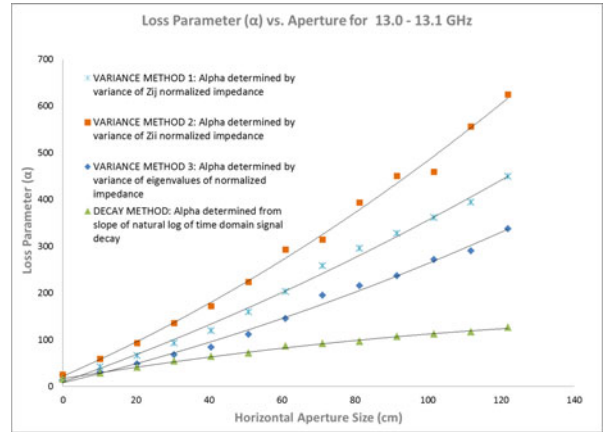


Fig. 6. Loss-parameter ( $\alpha$ ) method evaluation results showing significant variation in  $\alpha$  as aperture size is increases from 0 to 121 cm.

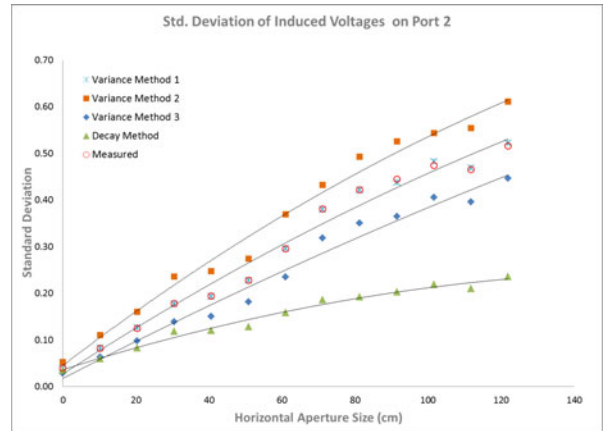


Fig. 7. Standard deviation of induced voltages on port 2. It can be seen that method 1 produces near-identical induced voltage statistics to those of the measured data (red circles).

**C. Data Analysis and Results**

Several methods for calculating the loss parameter of an enclosure are considered here, namely, the decay method and three types of the impedance-variance method [12], [13]. The decay method uses (1) as the general expression for the calculation of the loss parameter  $\alpha$ . The loaded quality factor  $Q$  is calculated from the time constant for energy decay inside the cavity (determined from the scattering parameters), but it is assumed that the volume remains well defined as the aperture is widened. The first two variance methods determine  $\alpha$  using only the variance of the measured normalized impedance matrix  $\bar{z}_{norm,ij}^{exp}$  or  $\bar{z}_{norm,ii}^{exp}$ . The third impedance-variance method determines  $\alpha$  by calculating the variance of the *eigenvalues* of the measured normalized impedance of the transmitting port using  $\alpha = 1/(\pi\lambda_z^{exp} \sigma_{norm,11}^2)$  [12]. There are other methods described in [12], but have not been considered here. All methods considered, with slight variations, work well for enclosures without apertures (see Fig. 6). However, as an aperture is introduced, and as the aperture size is increased, we find that each method produces a different estimate of  $\alpha$ , as shown in Fig. 6. Note that the decay method is the only one that suggests the loss parameter saturates at large aperture sizes. This is likely due to

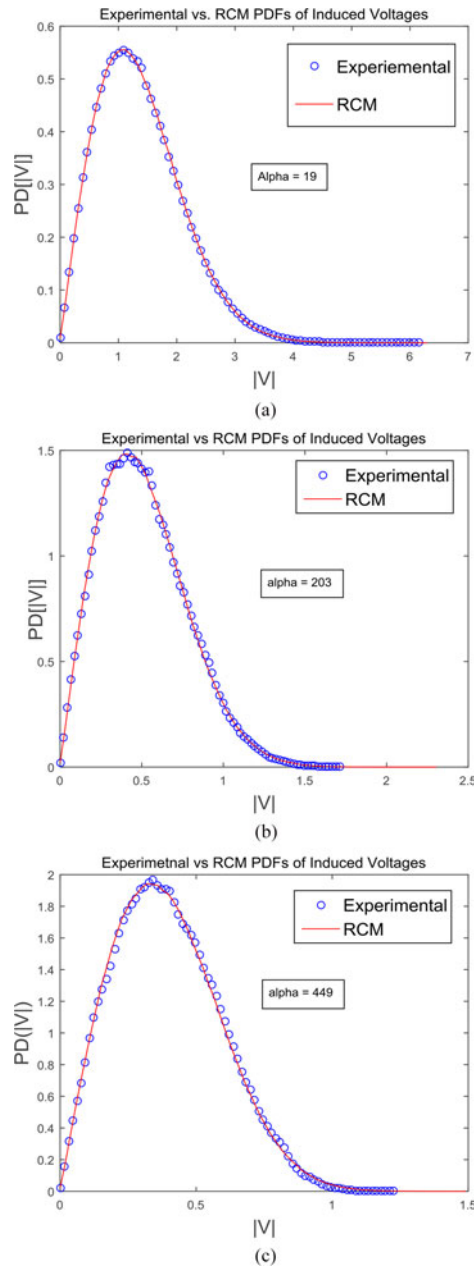


Fig. 8. Comparison of measured and RCM-predicted induced voltage PDFs for aperture widths of (a) 0 cm, (b) 61 cm, and (c) 121 cm, respectively. PDFs shown are for the 13.0 to 13.1 GHz band, similar results were obtained for the higher bands of 13.4–13.5 GHz, and 13.9–14.0 GHz. Note: axes are not identical across figures as they are meant only for showing goodness of fit.

the fact that the loss parameter also explicitly scales with the system size, and this effect is not included in the decay method.

Further, all methods produce a loss parameter value which leads to RCM-predicted statistics that deviate from the experimentally determined statistics, with the exception of the statistics of the variance of the normalized impedance of  $\bar{z}_{\text{norm},ij}^{\text{exp}}$ . Fig. 6 shows that there is variability in the predicted standard deviation of the induced voltage distribution for the different  $\alpha$  values determined using the four methods described. It is clear that there is reduced variability in the induced voltage distribution standard deviation for an enclosure with no apertures. In order to determine which  $\alpha$  value provides the best fit

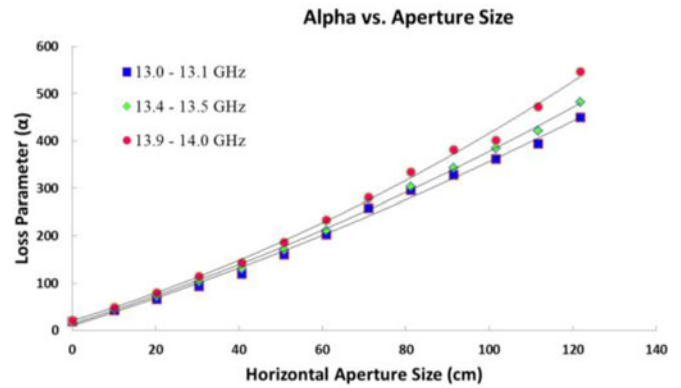


Fig. 9. Loss parameter values were obtained by method 1 versus aperture size. The maximum horizontal aperture length was 122 cm and vertical aperture height was a constant 30.5 cm.

for all aperture sizes, we can examine the standard deviation of the induced voltages determined from experimental data and compare the values with those from the RCM-predicted induced voltages generated using the  $\alpha$  values from the different methods. Fig. 7 shows that only method 1 produces a good fit with the PDFs calculated from measured data, and the goodness of fit to the entire PDF can be seen visually in Fig. 8.

Fig. 8 shows three comparisons of measured versus RCM-predicted (using variance method 1) induced voltage distributions for three different aperture widths. There is good agreement between the experimental and RCM-predicted PDFs for several aperture sizes when using the  $\alpha$  value obtained from variance of the normalized impedance matrix  $\bar{z}_{\text{norm},ij}^{\text{exp}}$ , method 1 in Figs. 6 and 7. Other determinations of  $\alpha$  predict induced voltage distributions that differ markedly from the data.

There is good agreement between the experimental and RCM-predicted PDFs for all three aperture sizes. Similar results are obtained for each of the other 100 MHz bands from 13.1 GHz to 14.0 GHz and other aperture sizes.

Fig. 9 shows the effect of aperture size and frequency variation on the loss parameter  $\alpha$  values, for method 1. One expects that the aperture becomes a more efficient radiator as its dimensions, in terms of the number of wavelengths, grows, and we see that as the aperture size is increased from a closed cavity to full aperture there is a corresponding increase in  $\alpha$ . There is also a trend toward increasing separation of  $\alpha$  values with increasing frequency for the frequency bands tested, as a function of aperture size.

#### IV. CONCLUSION

Previous work has shown that the RCM can be used to accurately predict induced voltages on a target port within a large complex enclosure without apertures when all radiations are internal to the enclosure. In this paper, we have shown that the RCM may also be used to predict induced voltages on a port in an enclosure with an electrically large aperture when the loss parameter  $\alpha$  is calculated using the variance of the normalized impedance matrix  $\bar{z}_{\text{norm},ij}^{\text{exp}}$ . Additionally, the frequency dependent nature of the loss parameter for the frequency band tested is demonstrated, and it is shown that as frequency is increased  $\alpha$  also increases. These results are applicable to electromagnetic compatibility concerns for electronics in both civilian and defense enclosures (buildings, ships, aircraft, etc.). Future work

will focus on studying RCM-induced voltage statistics predictions in aperture-connected enclosures, as well as the effect of scaling in frequency, enclosure size, and conductivity.

## REFERENCES

- [1] D. A. Hill, *Electromagnetic Fields in Cavities: Deterministic and Statistical Theories*. New York, NY, USA: Wiley, 2009.
- [2] D. Fedeli, G. Gradoni, V. M. Primiani, and F. Moglie, "Accurate analysis of reverberation field penetration into an equipment-level enclosure," *IEEE Trans. Electromagn. Compat.*, vol. 51, no. 2, pp. 170–180, May 2009.
- [3] Y. He and A. C. Marvin, "Aspects of field statistics inside nested frequency-stirred reverberation chambers," presented at the IEEE Int. Symp. Electromagnetic Compatibility, Austin, TX, USA, Aug. 2009.
- [4] G. B. Tait, R. E. Richardson, M. B. Slocum, M. O. Hatfield, and M. J. Rodriguez, "Reverberant microwave propagation in coupled complex cavities," *IEEE Trans. Electromagn. Compat.*, vol. 53, no. 1, pp. 229–232, Feb. 2011.
- [5] G. B. Tait, C. Hager, M. B. Slocum, and M. O. Hatfield, "On measuring shielding effectiveness of sparsely moded enclosures in a reverberation chamber," *IEEE Trans. Electromagn. Compat.*, vol. 55, no. 2, pp. 231–240, Apr. 2013.
- [6] H.-J. Stockmann, *Quantum Chaos: An Introduction*. Cambridge, UK: Cambridge Univ. Press, 1999.
- [7] R. Holland and R. St. John, *Statistical Electromagnetics*. Philadelphia, PA, USA: Taylor & Francis, 1999.
- [8] Z. B. Drikas *et al.*, "Application of the random coupling model to the calculation of electromagnetic statistics in complex enclosures," *IEEE Trans. Electromagn. Compat.*, vol. 56, no. 6, pp. 1480–1487, Dec. 2014.
- [9] T. M. Antonsen, G. Gradoni, S. Anlage, and E. Ott, "Statistical characterization of complex enclosures with distributed ports," presented at the IEEE Int. Symp. Electromagnetic Compatibility, Long Beach, CA, USA, 2011.
- [10] X. Zheng, T. M. Antonsen, and E. Ott, "Statistics of impedance and scattering matrices in chaotic microwave cavities: Single channel case," *Electromagnetics*, vol. 26, no. 1, pp. 3–35, Feb. 2006.
- [11] X. Zheng, T. M. Antonsen, Jr., and E. Ott, "Statistics of impedance and scattering matrices of chaotic microwave cavities with multiple ports," *Electromagnetics*, vol. 26, pp. 37–55, 2006.
- [12] S. Hemmady, "The random coupling model: A wave-chaotic approach to predicting and measuring electromagnetic field quantities in complicated enclosures," Ph.D. dissertation, Univ. Maryland, College Park, MD, USA, 2006.
- [13] S. Hemmady, E. Ott, S. M. Anlage, and T. M. Antonsen, "Statistical prediction and measurement of induced voltages on components within complicated enclosures: A wave-chaotic approach," *IEEE Trans. Electromagn. Compat.*, vol. 54, no. 4, pp. 758–771, Aug. 2012.
- [14] O. Bohigas, M. J. Gionnoni, and C. Schmidt, "Characterization of chaotic quantum spectra and universality of level fluctuation laws," *Phys. Rev. Lett.*, vol. 52, no. 1, pp. 1–4, Jan. 1984.
- [15] J. A. Hart, T. M. Antonsen, and E. Ott, "The effect of short ray trajectories on the scattering statistics of wave chaotic systems," *Phys. Rev. E*, vol. 80, 2009, Art. no. 041109.
- [16] J.-H. Yeh, J. Hart, E. Bradshaw, T. Antonsen, E. Ott, and S. M. Anlage, "Experimental examination of the effect of short ray trajectories in two-port wave-chaotic scattering systems," *Phys. Rev. E*, vol. 82, 2010, Art. no. 041114.
- [17] S. Hemmady, X. Zheng, E. Ott, S. M. Anlage, and T. Antonsen, "Universal statistics of the scattering coefficient of chaotic microwave cavities," *Phys. Rev. E*, vol. 71, 2005, Art. no. 056215.



**Jesus Gil Gil** received the B.S. and M.S. degrees in electrical engineering from George Mason University, Fairfax, VA, USA, in 2005 and 2008, respectively.

He is currently an Electrical Engineer at the High Power Microwave Section of the US Naval Research Laboratory. His research interests include Chaos in electronics, the random coupling model, metamaterials, nonlinear behavior in semiconductors, and high power microwaves. He has coauthored peer-reviewed publications on the random coupling, and has given

numerous presentations at the Annual Symposium of the Directed Energy Professional Society.



**Zachary B. Drikas** (S'07–M'13) received the B.S. and M.S. degrees in electrical engineering from the George Washington University, Washington, DC, USA, in 2011 and 2012, respectively.

He is currently working with the High Power Microwave Section at the US Naval Research Laboratory. He has co-authored peer-reviewed publications on the random coupling model and electromagnetic time-reversal techniques, and he has given numerous presentations at the Annual Symposium of the Directed Energy Professional Society. His research interests include investigating high power microwave effects on electronics, nonlinear behavior in semiconductors, electromagnetic time-reversal techniques, and using the random coupling model to characterize and predict effects on targets in ray-chaotic enclosures.



**Tim D. Andreadis** received the B.S. degree in physics and the Ph.D. degree in nuclear engineering both from the University of Maryland, College Park, MD, USA, in 1974 and 1981, respectively.

He is currently the Head of the High Power Microwave (HPM) section at the US Naval Research Laboratory, Washington, DC, USA. He has an extensive list of peer-reviewed publications, conference proceedings, and reports. He has numerous invited talks and presentations at national and international conferences. His research interests include HPM effects on electronics, counter IED applications, high power RF source applications, and electromagnetic backscatter.

Dr. Andread is a Fellow of the Directed Energy Professional Society.



**Steven M. Anlage** (M'94) received the B.S. degree in physics from the Rensselaer Polytechnic Institute, Troy, NY, USA, in 1982, and the M.S. and Ph.D. degrees in applied physics from the California Institute of Technology, Pasadena, CA, USA, in 1984 and 1988, respectively.

He is a Professor of physics and Faculty Affiliate at the Department of Electrical and Computer Engineering, University of Maryland, College Park, MD, USA. His graduate work concerned with the physics and materials properties of quasicrystals. His postdoctoral work with the Beasley-Geballe-Kapitulnik group at the Stanford University (1987–1990) concentrated on high-frequency properties of high-temperature superconductors, including both basic physics and applications to tunable microwave devices. In 1990, he was appointed as an Assistant Professor of physics in the Center for Superconductivity Research, University of Maryland, then Associate Professor in 1997, and finally Full Professor of physics in 2002. He was the interim Director of the Center for Nanophysics and Advanced Materials (2007–2009), and is a Member of the Maryland NanoCenter. His research in high-frequency superconductivity has addressed questions of the pairing state symmetry of the cuprate superconductors, the dynamics of conductivity fluctuations and vortices, and microwave applications such as superconducting negative index of refraction metamaterials. He has also developed and patented a near-field scanning microwave microscope for quantitative local measurements of electronic materials (dielectrics, semiconductors, metals, and superconductors) down to nm length scales. He has also performed microwave analog experiments of the Schrödinger equation to test fundamental theories of quantum chaos. As a part of this work he has developed a statistical prediction model for effects of high-power microwave signals on electronics. He is also active in the emerging field of time-reversed electromagnetics. His research is funded by the National Science Foundation, DoE and DoD, and he is an active Consultant of the US Government. In 2008, he was appointed as a Research Professor of the National Security Institute at the Naval Postgraduate School in Monterey, CA. In 2011, he was appointed as a Visiting Professor at the Center for Functional Nanostructures, Karlsruhe Institute of Technology, Germany. He has coauthored more than 180 research papers in scientific journals.

Dr. Anlage is a Member of the American Physical Society, the Optical Society of America, and the Materials Research Society.